Biochimica et Biophysica Acta 1864 (2016) 1539–1547

Contents lists available at ScienceDirect

Biochimica et Biophysica Acta

journal homepage: www.elsevier.com/locate/bbapap

Comparative functional characterization of eugenol synthase from four different *Ocimum* species: Implications on eugenol accumulation

Atul Anand [a,b], Ramesha H. Jayaramaiah [a], Supriya D. Beedkar [a,b,c], Priyanka A. Singh [a,b], Rakesh S. Joshi [d], Fayaj A. Mulani [b], Bhushan B. Dholakia [a], Sachin A. Punekar [e], Wasudeo N. Gade [c], Hirekodathakallu V. Thulasiram [b,f,*], Ashok P. Giri [a,**]

[a] Plant Molecular Biology Unit, Division of Biochemical Sciences, CSIR-National Chemical Laboratory, Pune 411008, Maharashtra, India
[b] Chemical Biology Unit, Division of Organic Chemistry, CSIR-National Chemical Laboratory, Pune 411008, Maharashtra, India
[c] Department of Biotechnology, Savitribai Phule Pune University (Formerly University of Pune), Pune 411007, Maharashtra, India
[d] Institute of Bioinformatics and Biotechnology, Savitribai Phule Pune University (Formerly University of Pune), Pune 411007, Maharashtra, India
[e] Biospheres, Eshwari, 52/403, Laxminagar, Parvati, Pune 411 009, Maharashtra, India
[f] CSIR-Institute of Genomics and Integrative Biology, Mall Road, New Delhi 110007, India

ARTICLE INFO

Article history:
Received 13 April 2016
Received in revised form 22 July 2016
Accepted 8 August 2016
Available online 09 August 2016

Keywords:
Eugenol
Chavicol
Eugenol synthase
Ocimum
Phenylpropanoids
Secondary metabolites

ABSTRACT

Isoprenoids and phenylpropanoids are the major secondary metabolite constituents in *Ocimum* genus. Though enzymes from phenylpropanoid pathway have been characterized from few plants, limited information exists on how they modulate levels of secondary metabolites. Here, we performed phenylpropanoid profiling in different tissues from five *Ocimum* species, which revealed significant variations in secondary metabolites including eugenol, eugenol methyl ether, estragole and methyl cinnamate levels. Expression analysis of eugenol synthase (*EGS*) gene showed higher transcript levels especially in young leaves and inflorescence; and were positively correlated with eugenol contents. Additionally, transcript levels of coniferyl alcohol acyl transferase, a key enzyme diverting pool of substrate to phenylpropanoids, were in accordance with their abundance in respective species. In particular, eugenol methyl transferase expression positively correlated with higher levels of eugenol methyl ether in *Ocimum tenuiflorum*. Further, EGSs were functionally characterized from four *Ocimum* species varying in their eugenol contents. Kinetic and expression analyses indicated, higher enzyme turnover and transcripts levels, in species accumulating more eugenol. Moreover, biochemical and bioinformatics studies demonstrated that coniferyl acetate was the preferred substrate over coumaryl acetate when used, individually or together, in the enzyme assay. Overall, this study revealed the preliminary evidence for varied accumulation of eugenol and its abundance over chavicol in these *Ocimum* species. Current findings could potentially provide novel insights for metabolic modulations in medicinal and aromatic plants.

1. Introduction

Phenylpropanoids, a group of plant secondary metabolites derived from phenylalanine, typically have propenyl side chains attached to a phenyl ring. These compounds are auto-toxic in nature and perform a vital role in plant communication, pollinator attraction and defense against herbivores and other pathogens [1–3]. Coniferyl and coumaryl alcohols are monolignol alcohol intermediates of the lignin biosynthetic pathway and serve as the precursors for phenylpropanoid biosynthesis. Biosynthesis of coumaryl alcohol involves coumaroyl-CoA reductase that acts on 4-coumaroyl-CoA to form 4-coumaraldehyde and provides a substrate for the synthesis of chavicol (Fig. 1). These alcohols are first converted to acetates by coniferyl- and coumaryl alcohol acyl transferases. The reductive elimination of the acetate moiety, which is catalyzed by eugenol synthase (EGS) yields the propenyl side chain. EGS utilizes coniferyl acetate and coumaryl acetate as substrates to produce eugenol and chavicol, respectively [4,5]. Methylation of eugenol and chavicol at the *para*-OH group of the phenyl ring is catalyzed by eugenol *O*-methyl transferase (EOMT) and chavicol *O*-methyl transferase (COMT) to form their methyl ether derivatives.

In this study, we have focused on EGS because eugenol has interesting properties like effector molecule in diabetes control [6] and is an important scent compound [7]. Till date, EGS has been characterized from few plant species such as *Ocimum basilicum (ObEGS1)* [4], *Gymnadenia odoratissima* [7], Petunia (PhEGS1), *Clarkia breweri*

* Correspondence to: H.V. Thulasiram, Chemical Biology Unit, Division of Organic Chemistry, CSIR-National Chemical Laboratory, Pune-411008 and CSIR-Institute of Genomics and Integrative Biology, Mall Road, New Delhi 110007, India.
** Corresponding author at: Plant Molecular Biology Unit, Division of Biochemical Sciences, CSIR-National Chemical Laboratory, Pune 411008.
E-mail addresses: hv.thulasiram@ncl.res.in (H.V. Thulasiram), ap.giri@ncl.res.in (A.P. Giri).

http://dx.doi.org/10.1016/j.bbapap.2016.08.004
1570-9639/

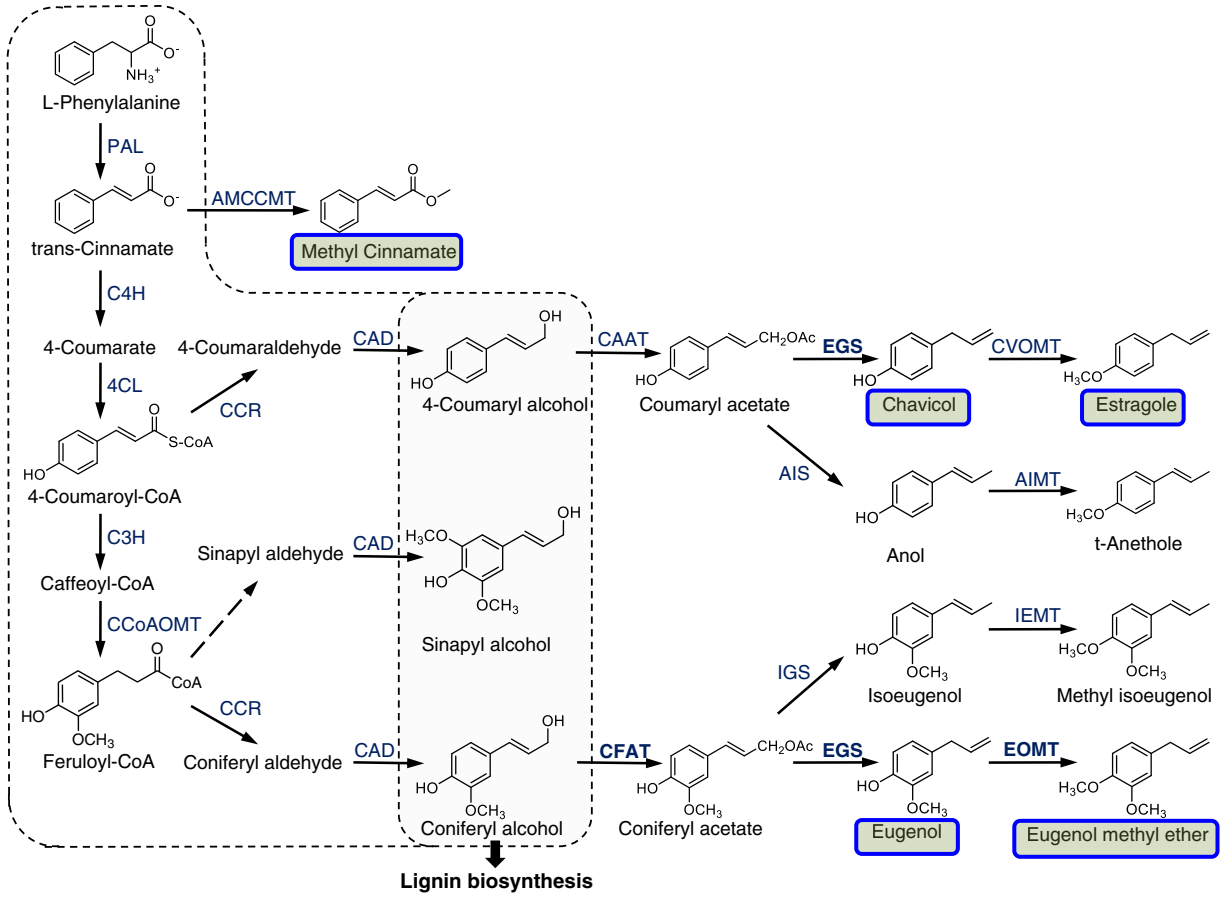

Fig. 1. Phenylpropanoid biosynthetic pathway showing identified metabolites (marked in box). In most plants, alternative reactions or enzymes are present. PAL, Phenylalanine ammonia lyase; C4H, trans-Cinnamate 4-hydroxylase; 4CL, 4-Coumarate CoA ligase; C3H, 4-Coumarate-3-hydroxylase; CCoAOMT, Caffeoyl-CoA *O*-methyl transferase; AMCCMT, S-adenosyl L-methionine Cinnamic acid carboxy methyl transferase; CCR, Cinnamoyl-CoA/coniferyl-CoA reductase; CAD, Coumaryl/coniferyl alcohol dehydrogenase; CAAT, 4-Coumaryl/Coniferyl alcohol acetyl transferase; EGS, Eugenol synthase; AS, anol synthase; CVOMT, chavicol *O*-methyl transferase; AOMT, anol *O*-methyl transferase, EOMT, eugenol *O*-methyl transferase.

(CbEGS1 and CbEGS2) [8] and *Pimpinella anisum* t-anol/isoeugenol synthase (PaAIS1) [9]. These enzymes belong to the pinoresinol isoflavone phenylcoumaran (PIP) family and perform NADPH-dependent reductases activity for the conversion of coniferyl acetate to eugenol [10]. EGS from *Larrea tridentata* (LtCES1) has been also shown to accept both coniferyl acetate and coumaryl acetate [5]. Although these reports describe about the characterization of EGS, very limited knowledge exists about the molecular basis for substrate selection and its effect on the modulation of secondary metabolites by EGS. Therefore, we performed phenylpropanoids profiling in different tissues from five *Ocimum* species and further functionally characterized EGSs from them. The kinetic parameters for these EGSs with coniferyl acetate indicated high turnover number of EGS in species having high eugenol content. Additionally, this was supported by *EGS* expression analysis indicating significant correlation between the *EGS* expression and eugenol levels. Though EGS could utilize two substrates, *in vitro* and *in silico* studies confirmed that eugenol was the predominantly detected phenylpropanoid while chavicol was present in trace amounts in assays when both the substrates were used together.

2. Materials and methods

2.1. Plant materials

Authenticated *Ocimum* plants belonging to five species, *Ocimum gratissimum* L. I and II (*Og*I and *Og*II), *O. tenuiflorum* L. I and II (*Ot*I and *Ot*II), *O. kilimandscharicum* Gürke (*Ok*), *O. americanum* L. (*Oa*) and *O. basilicum* L. I, II, III and IV (*Oba*I, *Oba*II, *Oba*III and *Oba*IV) were grown in a greenhouse at 25–28 °C with ~35–40% humidity and 16 h light and 8 h dark periods. Plant samples of all the species were deposited in the herbarium of Botanical Survey of India, Pune as voucher specimens. All the samples were collected from 2 to 3 months old plants, immediately frozen in liquid nitrogen and stored at −80 °C until further use. Fresh tissues were used for metabolite extraction and analysis.

2.2. Chemicals and substrates

All chemicals were purchased from Sigma-Aldrich (Sigma Chemical Co., USA), unless stated. Coniferyl acetate and coumaryl acetate were synthesized from coniferyl alcohol and coumaryl alcohol, respectively, as previously described [2]. The procedure for synthesizing coumaryl alcohol and chavicol is detailed in supplementary data set 1. The TA cloning kit with pCR 2.1 vector, pET102 directional cloning kit, PCR purification kit, gel extraction kit and Accuprime proof reading polymerase were purchased from Thermo Scientific (USA).

2.3. Analysis of phenylpropanoids from different Ocimum species

Phenylpropanoid abundance was measured in six different tissues including young leaves (YL; top whorl), mature leaves (ML; third whorl), inflorescence (I), flower (F), stem (S) and root (R) from five *Ocimum* species. Extractions were performed by dichloromethane (DCM) extraction method, as reported previously [11]. Briefly, fresh tissues (5 g each) from different plant parts were harvested separately and immediately soaked in 50 mL DCM for 20 h at 28 °C. The combined organic phase was cooled to −20 °C for 2 h (for lipid precipitation) and

filtered. The contents were dried, weighed, re-dissolved in 2 mL DCM and subjected to GC and GC–MS analyses was carried out for 3 biological replicates in triplicates. GC analyses were carried out on an Agilent 7890 A instrument equipped with a hydrogen flame ionization detector and HP-5 capillary column (30 m × 0.32 mm × 0.25 μm, J and W Scientific, USA). Nitrogen was used as the carrier gas at a flow rate of 1 mL/min. The column temperature was raised from 70 °C to 110 °C at 2 °C min^{-1}, then raised to 180 °C at 3 °C min^{-1} and finally at 10 °C min^{-1} raised to 220 °C and held for 2 min. Injector and detector temperatures were 230 °C and 235 °C, respectively. GC–MS was performed on an Agilent 5975C mass selective detector interfaced with an Agilent 7890 A gas chromatograph using an HP-5 MS capillary column with helium as the carrier gas and using above mentioned conditions. Compounds were identified by co-injection studies, comparing the retention time and mass fragmentation pattern with those of reference compounds and also compared acquired mass spectra and retention indices with those of NIST/NBS and the Wiley mass spectral library (software version 2.0, Dec. 2005).

2.4. RNA isolation, semi-quantitative and quantitative RT-PCR

Total RNA was extracted from the different tissues using Spectrum™ Plant Total RNA Isolation Kit (Sigma Chemical Co., USA). The DNase-treated RNA (4 μg) was used for cDNA preparation in a 20 μL reaction using SuperScript™ III reverse-transcriptase system (Thermo Scientific). Semi-quantitative RT-PCR (sqRT-PCR) was performed for *EGS*, eugenol o-methyl transferase (*EOMT*) and coniferyl alcohol acyl transferase (*CFAT*) in 10 μL reactions consisting of 5 μL of 2X Jumpstart readymix, 1 μL each of 10 μM gene specific forward and reverse primers, 1 μL of cDNA optimized with endogenous control (18S rRNA) and nuclease free water was added to a volume of 10 μL. PCR was carried out for 30 cycles and the amplified products were run on 1% agarose gel. Quantitative RT-PCR (qRT-PCR) was performed by using Taqman chemistry. A typical reaction consisted of 5 μL of Taqman advanced master-mix, 0.5 μL of primer-probe mix and 1 μL of diluted cDNA (1:2) with nuclease-free water added to make up a volume of 10 μL. For qRT-PCR reactions, actin was used as an endogenous control and the reactions were carried out in triplicates for 3 biological replicates in the 7500 Fast Real Time PCR System (Thermo Scientific). Annealing temperature was kept at 60 °C and cycling conditions were kept as per the manufacture's instruction. Primer sequences, and assay identification number for Taqman primer–probes were as given in (Supplementary Table S1).

2.5. Isolation of EGS from ten Ocimum subtypes and sequence analysis

5′ and 3′ RACE PCR was performed by using primers (Supplementary Table S1) designed from the reported ObEGS1 nucleotide sequence (Accession no. DQ372812). RACE cDNA was prepared from 5 μg of total RNA from the leaf tissue using the Generacer kit (Thermo Scientific). RACE PCR products were cloned in the pCR 2.1 vector and transformed into TOP10 cells. Sequence verified RACE fragments were used to generate open reading frame for EGS. EGSs from five species were isolated by using terminal primers and similarly cloned, sequenced and their sequences have been submitted to NCBI (GenBank accession no. KU977432-KU977441). For cloning *EGS*s into pET 102 expression vector, 5′-CACC-3′ was added to the 5′ end of the forward primer, and in reverse primer stop codons were removed to allow for C-terminal 6X His-tag expression. The sequence analyses were carried out on Bioedit software (Ibis Biosciences, USA); alignment was done using the CLUSTALW2 program (http://www.ebi.ac.uk/Tools/msa/clustalw2/). Nucleotide sequences were translated using the ExPASy translate tool (http://web.expasy.org/translate/) and BOXSHADE 3.21 (http://www.ch.embnet.org/software/BOX_form.html) was used for marking identical and similar amino acid residues. Multiple alignments of EGS sequences were done using CLUSTALW2, and the neighbor-joining tree was constructed (with 1000 bootstrap value) using MEGA6 [12].

2.6. Expression, purification and enzyme assay of recombinant EGS

Plasmid of the pET 102 harboring full-length transcripts of *EGS* was introduced into Rosetta 2 (DE3) chemically competent cells. A single colony was inoculated in 5 mL of Luria Bertani broth (LB) and incubated on a rotary shaker (200 rpm) at 37 °C for 12 h. This culture was used for inoculating 50 mL "terrific broth" (TB) in a 250 mL Erlenmeyer flask and incubated on a rotary shaker (200 rpm) at 37 °C till optical density reached 0.6–0.8. The culture was induced with 1 mM Isopropyl β-D-1-thiogalactopyranoside (IPTG) and incubated on a rotary shaker for 12 h at 18 °C. After incubation cells were pelleted by centrifugation and purification was carried out as described in Supplementary data S2.

Enzyme activity was measured by GC-FID as described previously [2,4]. The assay mixture (200 μL) consisted of 50 mM MES buffer (pH 6.5), 1 mM coniferyl acetate/ coumaryl acetate/cinnamyl acetate and 20 μg of purified protein. The enzyme reaction was initiated by adding 1 mM NADPH. The mixture was incubated at 25 °C for 30 min. After this incubation period, the assay contents were cooled to 4 °C on ice and then linalool (1 μg) as an internal standard and NaCl (~200 mg) were added. The assay contents were extracted with DCM (1 mL × 3). The combined organic phase was dried over anhydrous sodium sulphate and concentrated to nearly 50 μL by flushing it with nitrogen. This extract (1 μL) was subjected to GC-FID and GC–MS analyses. For kinetic experiments, substrate concentrations ranged from 0.1 to 5 mM.

2.7. Modeling and docking analysis

Homology models for OgIEGS, ObaIEGS, OtIEGS and OkEGS were constructed with SwissModel server (http://swissmodel.expasy.org/) using the structure of EGS-NADP + EMDF complex (PDB ID: 2QZZ). Energy minimization of predicted models was done with GROMOS96 force field using Swiss PDB viewer (http://spdbv.vital-it.ch/). Modelled structures were validated by RAMPAGE (http://mordred.bioc.cam.ac.uk/~rapper/rampage.php), Molprobity (http://molprobity.biochem.duke.edu/) and ProSA analysis (https://prosa.services.came.sbg.ac.at/prosa.php). AutoDock 4.2 software (http://autodock.scripps.edu/) was used to convert receptor and ligand from *.pdb to *.pdbqt format and to set other docking parameters. The grid map was set around the Lys132 residue of EGS. Initially, two catalytic water molecules were docked in the active site. EGS with catalytic water molecules was taken for further docking with substrates *i.e.* cinnamyl, coumaryl and coniferyl acetates. The structure of the EGS + NADP + substrate complex was further optimized by energy minimization in Swiss PDB viewer (http://spdbv.vital-it.ch/). Complexes were analyzed for polar contact in the binding pocket using PyMol (https://www.pymol.org/).

2.8. Statistical analysis

All the metabolite and gene expression analyses were carried out with three biological and three technical replicates each. Data sets were represented as mean ± standard deviation. Significant differences between samples for gene expression analysis were performed with two-way ANOVA followed by Bonferroni's multiple comparisons test.

3. Results

3.1. Distribution of phenylpropanoids in different tissues of Ocimum species

The GC-FID and GC–MS analyses of the metabolite extracts from different tissues of various *Ocimum* species indicated the presence of at least six major phenylpropanoids with significant variation in their distribution across five species (Table 1). Predominantly, we detected end products of the phenylpropanoid pathway that were active in

Table 1
Levels of phenylpropanoids in different tissues of five *Ocimum* species.

Species	Tissues	Level of phenylpropanoids [ng/g of fresh weight (FW) ± SE]					
		Eugenol	Eugenol methyl ether	Chavicol	Estragole	Cis-methylcinnamate	Trans-methylcinnamate
Og I	YL	15,106.43 ± 26.72	ND	7.68 ± 0.33	ND	ND	ND
	ML	11,692.18 ± 82.45	ND	5.57 ± 0.04	ND	ND	ND
	I	9229.38 ± 14.92	ND	8.32 ± 0.51	ND	ND	ND
	F	9911.74 ± 8.48	ND	8.53 ± 0.19	ND	ND	ND
	S	1414.12 ± 2.97	ND	1.32 ± 0.11	ND	ND	ND
	R	53.61 ± 1.68	ND	ND	ND	ND	ND
Og II	YL	14,942.73 ± 147.1	ND	ND	ND	ND	ND
	ML	5192.45 ± 45	ND	ND	ND	ND	ND
	I	4178.02 ± 5.6	ND	ND	ND	ND	ND
	F	3329.96 ± 0.04	ND	ND	ND	ND	ND
	S	364.21 ± 22.6	ND	ND	ND	ND	ND
	R	53.08 ± 21	ND	ND	ND	ND	ND
Ot I	YL	212.76 ± 0.54	5653.86 ± 11.52	ND	ND	ND	ND
	ML	489.6 ± 0.41	2037.41 ± 2.17	ND	ND	ND	ND
	I	237.6 ± 3.22	2376.26 ± 31.54	ND	ND	ND	ND
	F	1003.88 ± 8.5	1212.21 ± 8.55	ND	ND	ND	ND
	S	351.75 ± 3.65	143.49 ± 3.88	ND	ND	ND	ND
	R	ND	ND	ND	ND	ND	ND
Ot II	YL	41.57 ± 2.2	7320.34 ± 30.78	ND	ND	ND	ND
	ML	386.97 ± 16	2676.53 ± 23.81	ND	ND	ND	ND
	I	59.52 ± 5.4	5818.25 ± 40.72	ND	3.86 ± 0.19	ND	ND
	F	90.39 ± 0.16	3988.1 ± 10.84	ND	ND	ND	ND
	S	119.59 ± 6.45	786.2 ± 10.28	ND	ND	ND	ND
	R	ND	ND	ND	ND	ND	ND
Ok	YL	3.39 ± 0.59	ND	ND	ND	ND	ND
	ML	4.11 ± 0.82	ND	ND	ND	ND	ND
	I	2.65 ± 0.98	ND	ND	ND	ND	ND
	F	ND	ND	ND	ND	ND	ND
	S	43.08 ± 13.16	ND	ND	ND	ND	ND
	R	967.88 ± 21.44	ND	ND	ND	ND	ND
Oa	YL	13.41 ± 0.6	ND	ND	ND	ND	ND
	ML	37.84 ± 17.81	ND	ND	ND	ND	ND
	I	3.76 ± 0.03	ND	ND	ND	ND	ND
	F	ND	ND	ND	ND	ND	ND
	S	47.16 ± 3.5	ND	ND	ND	ND	ND
	R	855.35 ±	ND	ND	ND	ND	ND
Oba I	YL	2.95 ± 0.23	24.6 ± 1.68	ND	50.61 ± 0.7	430.28 ± 2	3250.07 ± 10.95
	ML	2.04 ± 0.43	10.05 ± 0.35	ND	17.62 ± 0.55	259.68 ± 1.28	1518.91 ± 5.19
	I	ND	24.75 ± 6.1	ND	225.49 ± 48.99	232.29 ± 3.73	7325.25 ± 28.57
	F	6.26 ± 0.54	8.28 ± 0.88	ND	37.13 ± 1.34	145.06 ± 3.21	2331.16 ± 10.85
	S	0.65 ± 0.01	1.54 ± 0.06	ND	ND	11.5 ± 0.03	27.93 ± 0.07
	R	ND	9.68 ± 0.1	ND	343.47 ± 3.22	ND	ND
Oba II	YL	3.28 ± 0.15	29.19 ± 0.67	10.86 ± 0.27	1735.77 ± 103.2	358.46 ± 27.94	2565.36 ± 67.72
	ML	5.15 ± 0.33	25.61 ± 1.56	3.54 ± 0.17	680.57 ± 72.26	443.29 ± 16.97	2769.87 ± 34.07
	I	ND	23.29 ± 1.42	ND	569.94 ± 18.61	237.99 ± 4.08	7645.68 ± 39.78
	F	ND	10 ± 1.39	ND	297.03 ± 18.74	150.09 ± 3.63	3877.79 ± 80.08
	S	2.21 ± 0.05	1.92 ± 0.06	2.52 ± 0.19	23.89 ± 0.91	12.11 ± 0.57	39.66 ± 1.66
	R	266.48 ± 3.12	ND	ND	ND	ND	59.62 ± 5.44
Oba III	YL	ND	7.91 ± 0.46	ND	26.72 ± 0.26	307.81 ± 4.61	2274.11 ± 35.98
	ML	ND	9.46 ± 0.53	ND	30.55 ± 2.06	422.5 ± 6.81	1509.08 ± 25.13
	I	ND	3.31 ± 0.25	ND	36.64 ± 7.01	177.04 ± 19.99	2772.45 ± 11.3
	F	ND	9.92 ± 1.06	ND	77.96 ± 8.15	310.73 ± 31.96	6221.9 ± 11.23
	S	12.36 ± 0.37	ND	ND	ND	6.2 ± 1.08	22.21 ± 1.08
	R	315.14 ± 5.15	ND	ND	ND	ND	ND
Oba IV	YL	ND	19.45 ± 1.75	ND	170.03 ± 1.54	272.09 ± 7.9	2746.56 ± 9.55
	ML	4.84 ± 0.14	1.07 ± 0.06	2.09 ± 0.05	2439.36 ± 6.96	ND	ND
	I	ND	6.72 ± 0.22	ND	724.76 ± 19.97	95.59 ± 1.53	2014.48 ± 33.3
	F	3.03 ± 0.2	2.74 ± 0.22	9.43 ± 0.45	3526.9 ± 10.87	ND	10.57 ± 0.34
	S	2.54 ± 0.03	ND	22.57 ± 0.33	151.75 ± 2.3	ND	ND
	R	112.58 ± 1.44	ND	ND	32.9 ± 2.92	ND	12.66 ± 1.07

ND = Not detected. The results shown are an average of three biological replicates ± standard errors.

respective *Ocimum* species (Fig. 1). In *Og*I, eugenol content varied from 15,106 ng/g of fresh weight (FW) in young leaves to 1414 ng/g of FW in stem (Table 1). In case of *Og*II, eugenol content was highest in young leaves (14,942 ng/g of FW) which showed lower levels in mature leaves (5192 ng/g of FW). Eugenol methyl-ether was detected only in *Ot*I and *Ot*II and was most abundant in young leaves with 5653 and 7320 ng/g in *Ot*I and II, respectively. Eugenol was also detected in *O. tenuiflorum* young and mature leaves, accounting for 213 ng/g to 490 ng/g of FW in *Ot*I, and 41 to 490 ng/g of FW in *Ot*II. Methyl cinnamate was a major phenylpropanoid in *Oba* subtypes, with its *trans* isomer being more abundant than *cis*. In *Oba*I, t-methyl cinnamate was present in varied concentrations among the different tissues ranging from 28 ng/g in stem to 7325 ng/g in inflorescence. In *Oba*III, *t*-methyl cinnamate was the principal component in flower (6221 ng/g of FW) and inflorescence in *Oba*II (7645 ng/g FW). Root tissues had trace levels of these compounds in most of these species.

3.2. Cloning and phylogenetic analysis of EGS from various Ocimum species

NCBI database search for EGS indicated a previously characterized EGS from *O. basilicum* (accession No: DQ372812), designated as ObEGS1. This sequence was used for *OgIEGS* cloning, which generated a 945 bp open reading frame (ORF) encoding 314 amino acids with an estimated molecular weight of 36 kDa. Similarly, nine EGS ORFs from other *Ocimum* species were also cloned and sequenced. Amino acid sequence alignments of EGSs indicated high sequence conservation among them. The lead residue, Lys132, was conserved in all the EGSs, with variations in residues lining both the active site (Phe85) and $NADP^+$ binding sites (Ser43) (Fig. 2). Phylogenetic analysis based on the neighbor-joining tree clustered these EGSs into four different groups. ObaIEGS and OkEGS formed a sub-cluster with reported ObEGS1 indicating evolutionary proximity among them (Fig. 3). The evolutionary relatedness of OgIEGS and OgII EGS (99% identity) and that of OaEGS, OtIEGS and OtIIEGS (97% identity) was also evident as they were in separate sub-cluster of EGSs.

3.3. Differential expression patterns of CFAT and EOMT result in varied levels of metabolites

The expression pattern of *CFAT*, responsible for diverting flux towards phenylpropanoid pathway, was analyzed in young leaf tissue of all five *Ocimum* species (Fig. 4A). Transcript levels of *CFAT* were highest in species accumulating eugenol (*Og*I) or eugenol methyl ether (*Ot*I), for which eugenol is the precursor molecule. In other species (*Ok*, *Oba*I and *Oa*), where eugenol levels were in traces, low levels of

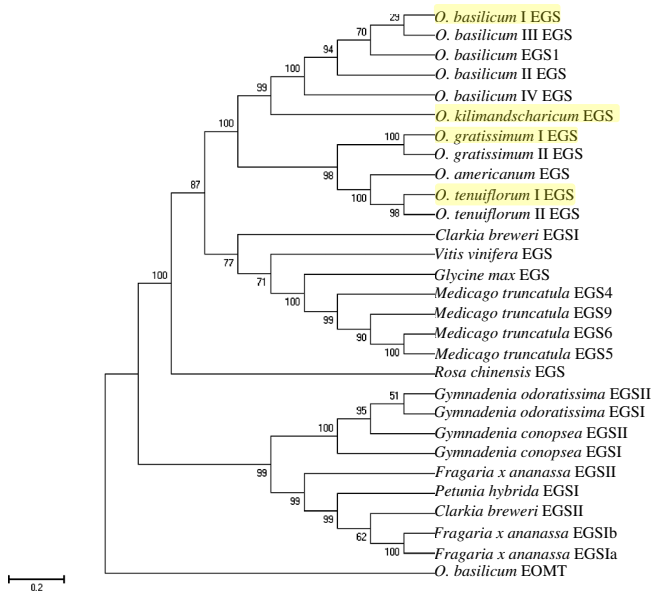

Fig. 3. Phylogenetic tree of four eugenol synthases (highlighted in yellow) with other reported sequences using MEGA6 with the bootstrap value of 1000 iterations. Total 29 EGS sequences were used to construct NJ tree with *Ocimum basilicum* Eugenol *O*-methyltransferase (AF435008) as an out group.

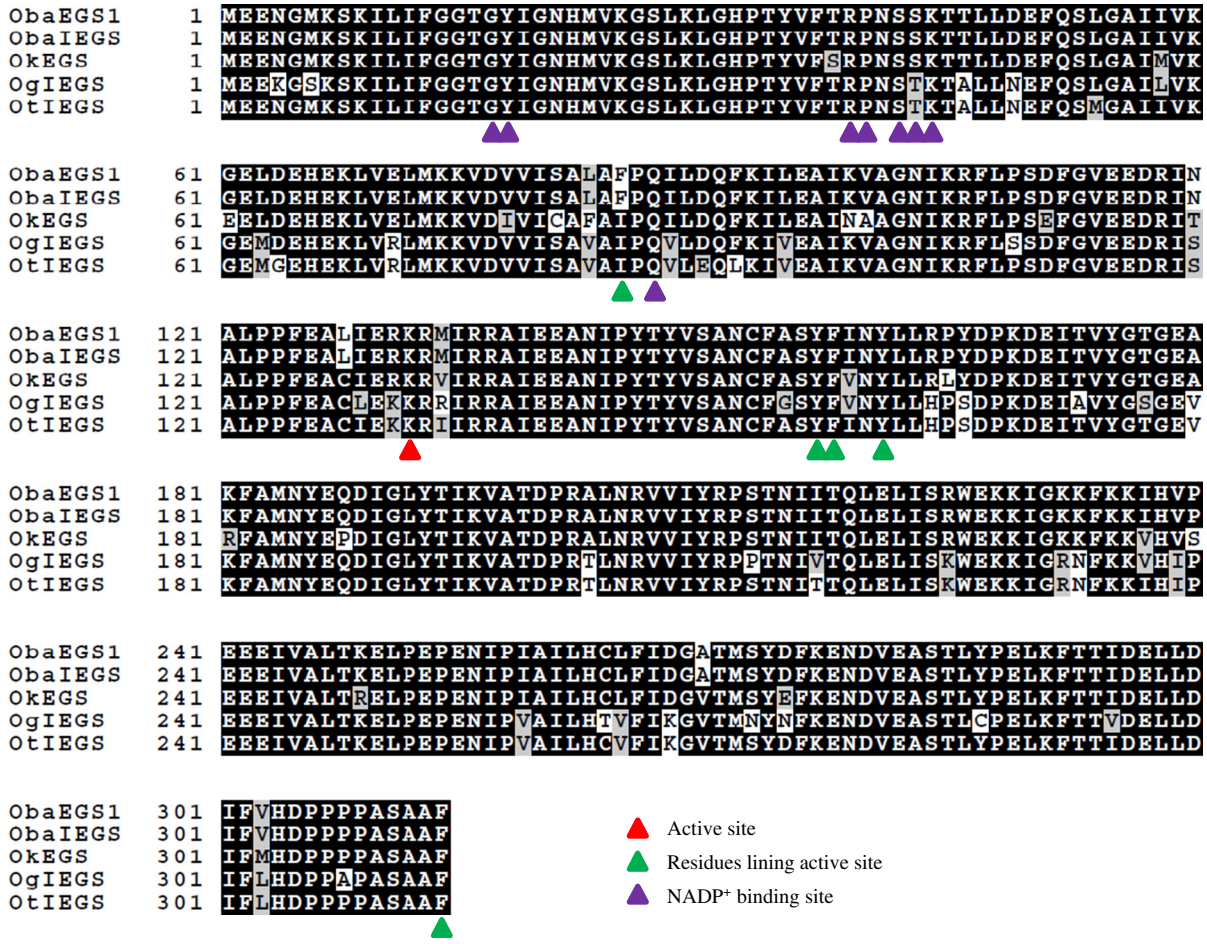

Fig. 2. Amino acid sequence alignment showing sequence conservation among eugenol synthases from five *Ocimum* species. Alignment was done by CLUSTALW and shaded using BOXSHADE 3.21. Identical residues are shaded black and similar residues are marked gray. The residues involved in substrate binding, phosphate binding, $NADP^+$ binding and active sites are indicated.

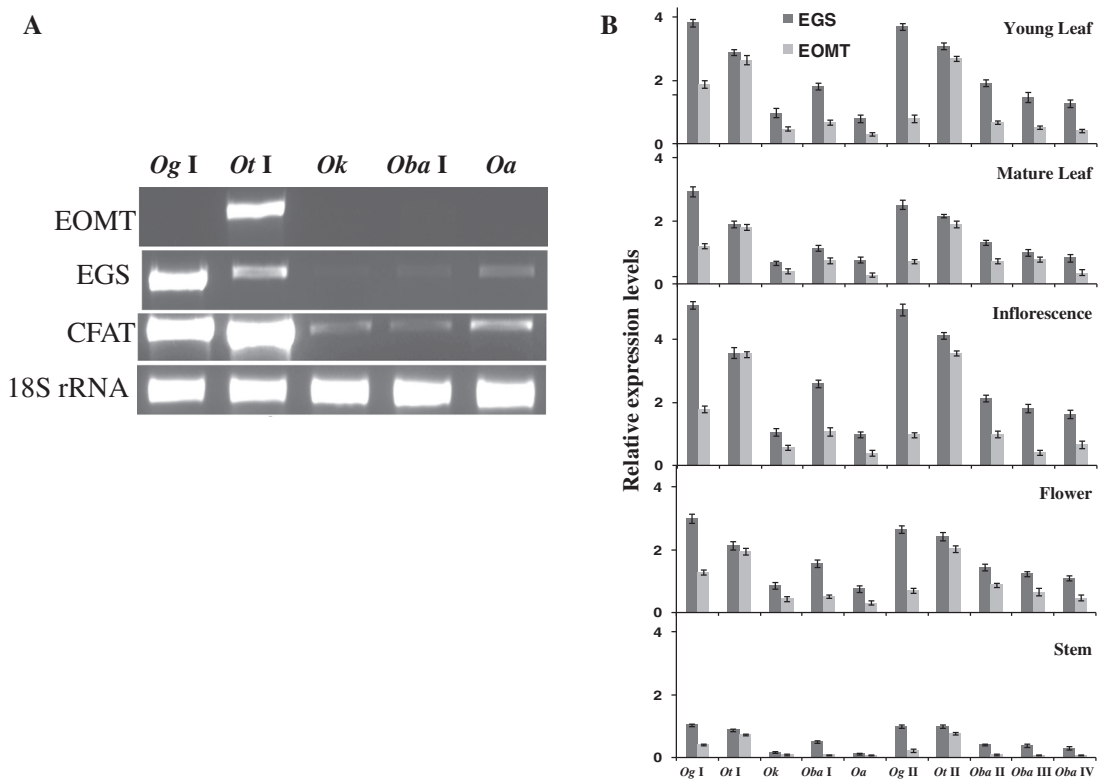

Fig. 4. Semi-quantitative real time PCR of *EGS*, *EOMT* and *CFAT* in young leaf tissue of all five species, with 18S rRNA as internal reference gene (A), qRT-PCR expression analyses of *EGS* and *EOMT* in different tissues from five *Ocimum* species (B). Absolute quantification was done by calculating the Ct values and normalizing the results with actin, the endogenous control. Bars represent the relative standard errors.

CFAT expression was evident. This suggested that expression of *CFAT* could be crucial for accumulation of eugenol or phenylpropanoids. Further, sqRT-PCR and qRT-PCR of *EOMT* indicated increased expression in *Ot*I (Fig. 4A) with high abundance in *Ot*I and *Ot*II (Fig. 4B), implying that *EOMT* expression might be responsible for the selective accumulation of eugenol methyl ether in *Ot*I and *Ot*II.

3.4. EGS expression pattern correlates with the eugenol levels

The expression level of *EGS* was determined by qRT-PCR in five tissues of different *Ocimum* species (Fig. 4B). These analyses showed a positive correlation between gene expression and eugenol levels. *EGS* expression was highest in young leaves and inflorescence tissues across

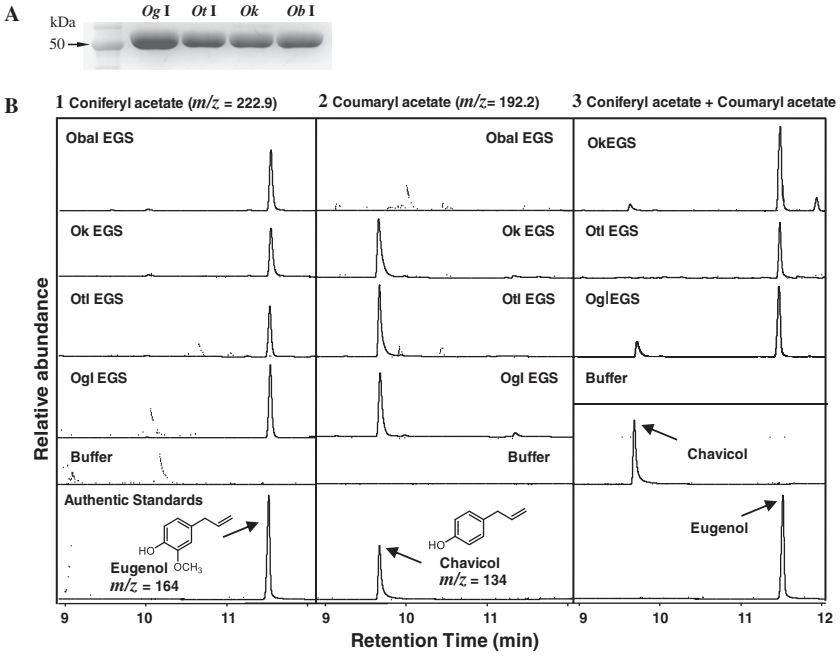

Fig. 5. His-tag purified and desalted recombinant EGS proteins run on 12% SDS-PAGE (A), characterization of recombinant EGS (B) – assay of rEGSs with 8 mM coniferyl acetate (1), assay of rEGSs with 8 mM coumaryl acetate (2), and assay of *Og*IEGS, *Ok*EGS and *Ot*IEGS with substrate mixed in K_m ratios (3).

all the *Ocimum* species, while stem had the lowest levels of *EGS*. The expression levels of *EGS* in mature leaves were lower than those in young ones. In *Ot*I and II, *EGS* expression levels were lower than that observed in *Og*I and II, which was consistent with the low levels of eugenol detected in these two species.

3.5. Substrate selectivity of recombinant EGS leads to high eugenol content

The recombinant EGSs were expressed and purified from four *Ocimum* species (Fig. 5A). Enzyme assays were performed using coniferyl acetate, coumaryl acetate and cinnamyl acetate as substrates with NADPH as a cofactor [1,4,13]. EGS showed catalytic activity towards coniferyl acetate and coumaryl acetate with different kinetic parameters (Fig. 5B and Table 2). Assays with buffer as control did not yield any product. For coniferyl acetate, the apparent K_m and k_{cat} values of OgIEGS were 0.5 mM and 0.68 min^{-1}, respectively, while these values were 1.2 mM and 0.2 min^{-1}, respectively for coumaryl acetate (Table 2). The kinetic parameters of OtIEGS, OkEGS and Oba*I*VEGS revealed similar biochemical characteristics. Comparison of coniferyl acetate with coumaryl acetate for their substrate affinity and turnover rate indicated that the former was the preferred substrate. When enzymatic assays were performed by mixing the two substrates in the ratio of their K_m values for respective EGS or in equi-molar concentration (1 mM each), a similar trend was observed. This was also in agreement with chemical profiling results confirming eugenol as the main phenylpropanoid over chavicol. However, EGS did not yield any product when cinnamyl acetate was used as a substrate.

3.6. Stable interaction between EGS and its substrates results in preferential eugenol accumulation

Three-dimensional structures of EGS showed similarity in structural attributes with other PIP-family proteins. EGS showed an N-terminal, Rossman-fold domain, containing a core, six-stranded parallel β-sheet flanked on each face by a helical layer. It had two important regions of catalytic function. First region was the binding pocket of active site, where a substrate's central scaffold attached leading to successful enzymatic reaction. β-sheet of the one core edge served as binding surface for the $NADP^+$ cofactor binding, while C-terminal domain was presumed to function in substrate binding. The examination of complex structure showed that in the binding pocket, the quinone-methide transition state was involved in cleaving the carbon-oxygen bond from the acetate moiety [14–16] and in serving as the actual substrate of the reduction reaction *via* NADPH-mediated hydride transfer (Fig. 6). Analysis of the polar contact network at the e-amino group of Lys132 indicated that the unprotonated -NH_2 state of this residue was the key donor in hydrogen-bond interactions with the hydroxyl group of the nicotinamide-ribose and the backbone carbonyl oxygen of Ser110. Furthermore, due to the electronegative nature of Lys132, it served as the acceptor in a hydrogen bond with the bridging water molecule and thus, acted as a general base. The de-protonation of *p*-hydroxyl group of the substrate was facilitated by its interaction with the water molecule (as a hydroxide ion). The second important region of catalytic function was the capping site of EGS active site, which was non-polar in nature. Tyr157 was a single residue available for hydrogen bond interactions with the polar oxygen atoms of the acetate moiety. The presence of aromatic side-chains in the lining region of the active site stabilized the binding of substrates.

All the variants of *Ocimum* EGS had similar three-dimensional structures. By superimposing OgI EGS, OkEGS, and OtIEGS on ObaIEGS, we observed that the active site was conserved, including the binding (Lys132) and capping regions (Tyr157) [17,18]. A docking study of various substrates (cinnamyl, coumaryl and coniferyl acetates) with OgIEGS, OtIEGS and ObaIEGS, indicated difference in binding energies (Table 3). This might be due to the variation in the residues that line active sites. Taken together, EGS binding to coniferyl acetate was relatively stronger than other substrates, coumaryl or cinnamyl acetate. In the case of coniferyl acetate, the presence of an additional hydroxymethyl group at the C3 position led to the formation of extra contact *via* attractive van-der-Waals force with lining residues. This might explain the strong binding of coniferyl acetate establishing it as the preferred substrate and thus, leading to more eugenol production than chavicol.

4. Discussion

Ocimum is a member of the mint family (Lamiaceae). Different *Ocimum* species have various combinations of phenylpropanoids, with eugenol and eugenol *O*-methyl ether being the most abundant in *O. gratissimum* and *O. tenuiflorum* species, while methyl cinnamate and estragole are more in *O. basilicum* species [5,19]. These compounds are synthesized in specialized structures (glandular trichomes), located on the aerial parts [20]. In the present study, eugenol, eugenol methyl ether, methyl cinnamate and estragole were identified as the major phenylpropanoids. Young plant tissue such as leaves and inflorescence had more phenylpropanoids than mature tissues that was consistent with their defensive role against pathogen attack and herbivory [5]. In mature leaves and flowers, substantial levels of these compounds were detected. The root tissue contained trace levels of these compounds, which could be transported through xylem and phloem [21]. There was extensive metabolite diversity, within and across different *Ocimum* species, *e.g.* selective presence of eugenol and eugenol methyl ether along with varied ratios of different phenylpropanoids in *Oba* species. The metabolite diversity across different species could be explained by the differential gene expression pattern (*e.g. EOMT* in *Ot*I and *Ot*II) resulting in accumulation of eugenol methyl ether. Consequently in other species, *EOMT* expression level was low leading to absence of this metabolite. Additionally, differences in metabolite profile could also be attributed to the post-translational modifications, whereby transcript abundance was not reflected in metabolite formation. For example, in *O. basilicum* var. SD, enzyme responsible for methylating chavicol was abundant but methylchavicol was not detected due to post-translation ubiquitylation of this enzyme [22]. Variations in metabolite accumulation within the species could be attributed to a number of factors. Differential gene expression of pathway enzymes and transcription factors could also bring these changes [23,24]. For instance, in two different varieties of *O. basilicum* SD and EMX-1,

Table 2
Values of kinetic parameters for four recombinant EGS.

Enzyme	Substrate	K_m (mM)	k_{cat} (min^{-1})	k_{cat}/K_m (mM^{-1} min^{-1})
*Og*IEGS	Coniferyl acetate	0.5 ± 0.04	0.68 ± 0.012	1.36
	Coumaryl acetate	1.25 ± 0.09	0. 2017 ± 0.012	0.16
*Ot*IEGS	Coniferyl acetate	1.17 ± 0.3	1.68 ± 0.25	1.44
	Coumaryl acetate	1.7 ± 0.2	0.8 ± 0.08	0.47
*Ok*EGS	Coniferyl acetate	0.41 ± 0.14	0.18 ± 0.013	0.44
	Coumaryl acetate	0.55 ± 0.2	0.63 ± 0.064	1.15
*Oba*IEGS	Coniferyl acetate	0.7 ± 0.02	0.23 ± 0.003	0.33
	Coumaryl acetate	ND	ND	

ND: Not detected. The results shown are an average of three technical replicates ± standard errors.

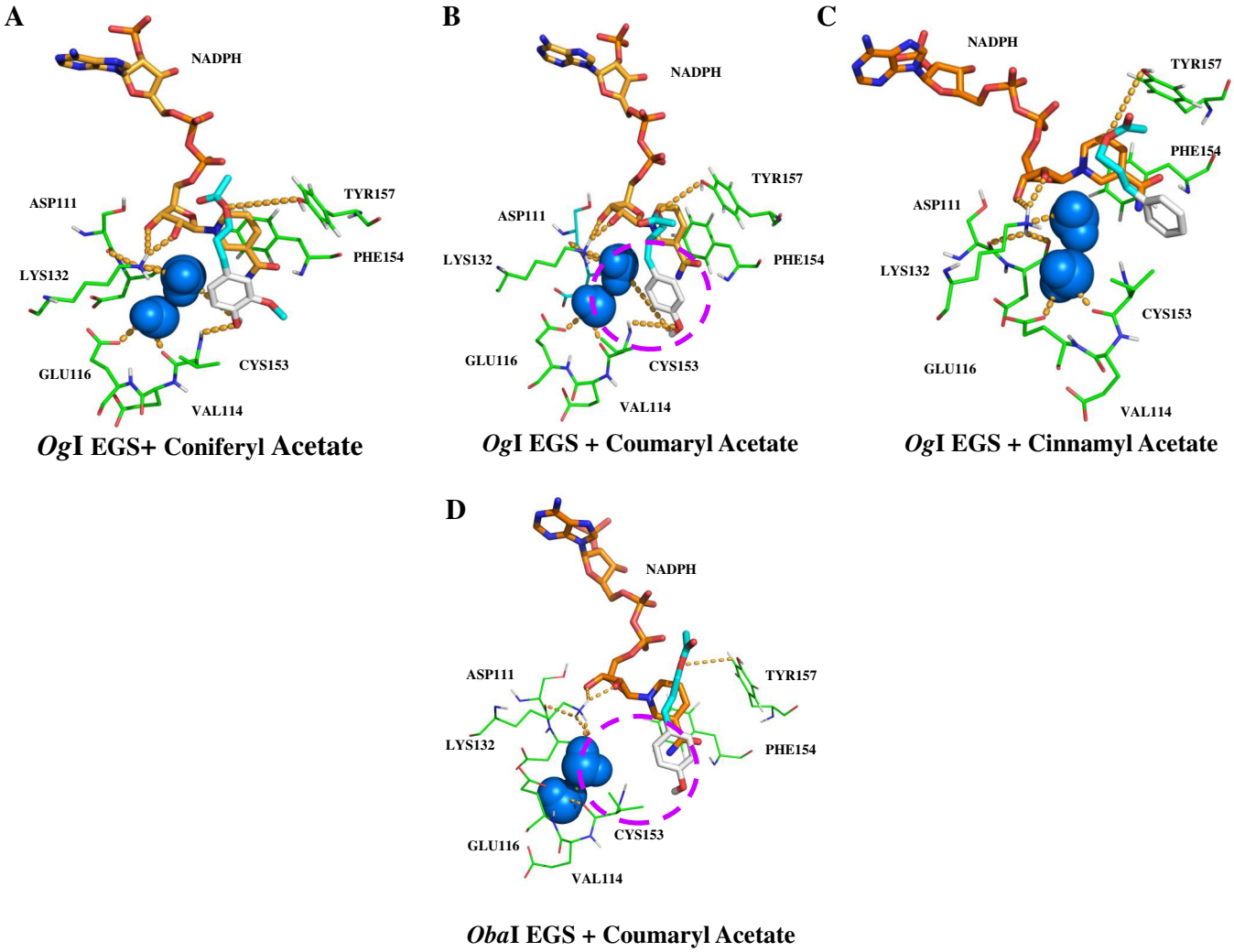

Fig. 6. Molecular docking of *Og*IEGS with different substrates. Interaction of active site lining residues of *Og*IEGS with coniferyl acetate (A), coumaryl acetate (B) and cinnamyl acetate (C). The standard atom coloring is used, with white carbon atoms for the substrates and orange carbons for NADPH. The close interaction between the binding pocket residues of *Og*IEGS, substrates and the hydride donor of the nicotinamide (C4) is shown as orange dashed line. Variation in the interaction of *Oba*IEGS with coumaryl acetate (D) as compared to *Og*IEGS is highlighted with dashed circle.

differential accumulation of phenylpropanoid was observed due to varied expression patterns of entry point enzymes, phenylalanine ammonia-lyase and 4-coumarate-CoA ligase [22].

EGS has been characterized in a number of plant species such as petunia, clarkia and strawberry [8,13]. In phylogenetic analysis, *Ocimum* EGSs were well separated from those of *Petunia hybrida*, *Clarkia breweri*, *Vitis vinifera* and *Medicago truncatula* that were grouped in separate sub-cluster. These 10 EGSs obtained from five *Ocimum* species were distributed in two sub-groups. Sequence comparison revealed that EGSs from different *Ocimum* species had high sequence conservation suggesting evolutionary proximity to EGS from other plants. *EGS* expression levels were positively correlated with the eugenol levels in different tissues from *Ocimum* species. *EGS* expression was highest in *Og*I and *Og*II, where eugenol was the major phenylpropanoid. Variation in *CFAT* expression levels, along with *EGS* and *EOMT* levels might be crucial for the selective eugenol accumulation among these *Ocimum* species. It has been reported that silencing of *CFAT* led to decreased accumulation of isoeugenol in petunia [25]. However, further experiments in terms of their *in planta* over-expression and silencing would be necessary to confirm their exact role. Characterizations and comparisons of four EGSs with coniferyl acetate and coumaryl acetate indicated that the former was the preferred substrate based upon its enzyme affinity, turnover number and catalytic efficiency. Additionally, when the substrates were mixed together either in equi-molar ratio or in the ratio of their K_m values, eugenol was the major product, with traces of chavicol detected in *Oba*I EGS and *Ot*I EGS. A homology model of EGS was made using the reported ObEGS1 structure as a template and interactions of both the substrates with the enzyme were analyzed. The lack of a hydroxymethyl substituent at the 3-position, as in the case of coumaryl acetate, significantly altered its stable interaction with EGS resulting in reduced preference as a substrate. In case of EGS from *Og*, *Ok* and *Ot*, coumaryl acetate made polar contact with catalytic water and Tyr157. Although with *Oba*I EGS, coumaryl acetate interacted through Tyr157, there was absence of polar interaction between coumaryl acetate and catalytic water, which might be one of the reasons for inactivity of EGS with it.

Table 3
Binding scores of EGS with three substrates.

Compound	Binding Score (kcal/mol)		
	*Og*IEGS	*Oba*IEGS	*Ot*IEGS
Coniferyl acetate	−7.6	−6.7	−6.9
Coumaryl acetate	−7.3	−6.6	−6.5
Cinnamyl acetate	−7.0	−6.4	−6.3

5. Conclusion

The present investigation provided better insight into the phenylpropanoids distribution in different tissues of five *Ocimum* species. Eugenol abundance was positively correlated with the *EGS* and expression levels of *CFAT* along with kinetic parameters of EGS revealed selective and higher eugenol accumulation than chavicol in these *Ocimum* species. Gene expression studies of *EOMT* provided evidence for its accumulation only in *O. tenuiflorum* species. Homology modeling and substrate docking clearly demonstrated the stable binding of coniferyl acetate making it as the preferred substrate compared to others. Taken together, these findings presented crucial insight for higher eugenol content in these *Ocimum* species and could be further utilized for metabolic manipulations in plants.

Conflict of interest

The authors declare that there are no conflicts of interest.

Transparency document

The Transparency document associated with this article can be found, in online version.

Acknowledgement

AA and PS acknowledge support from Council of Scientific and Industrial Research (CSIR), New Delhi. SB and RJ acknowledge support from University Grants Commission, New Delhi, India for Senior Research and the Kothari Fellowships, respectively. The work was funded by CSIR-NCL-IGIB Joint Research program under XII Five Year Plan (BSC0124). The authors acknowledge Ms. Emily Wheeler, Jamaica Plain, MA, USA for editorial assistance.

Appendix A. Supplementary data

Supplementary data to this article can be found online at http://dx.doi.org/10.1016/j.bbapap.2016.08.004.

References

[1] D.R. Gang, J. Wang, N. Dudareva, K.H. Nam, J.E. Simon, E. Lewinsohn, E. Pichersky, An investigation of the storage and biosynthesis of phenylpropenes in sweet basil, Plant Physiol. 125 (2001) 539–555.
[2] G.V. Louie, T.J. Baiga, M.E. Bowman, T. Koeduka, J.H. Taylor, S.M. Spassova, E. Pichersky, J.P. Noe, Structure and reaction mechanism of basil eugenol synthase, PLoS One 2 (2007), e993.
[3] M.J. Reigosa, E. Pazos-Malvido, Phytotoxic effects of 21 plant secondary metabolites on *Arabidopsis thaliana* germination and root growth, J. Chem. Ecol. 33 (2007) 1456–1466.
[4] T. Koeduka, E. Fridman, D.R. Gang, D.G. Vassao, B.L. Jackson, C.M. Kish, I. Orlova, S.M. Spassova, N.G. Lewis, J.P. Noel, T.J. Baiga, N. Dudareva, E. Pichersky, Eugenol and isoeugenol, characteristic aromatic constituents of spices, are biosynthesized via reduction of a coniferyl alcohol ester, Proc. Natl. Acad. Sci. U. S. A. 103 (2006) 10128–10133.
[5] D.G. Vassao, D.R. Gang, T. Koeduka, B. Jackson, E. Pichersky, L.B. Davin, N.G. Lewis, Chavicol formation in sweet basil (*Ocimum basilicum*): Cleavage of an esterified C9 hydroxyl group with NAD(P)H-dependent reduction, Org. Biomol. Chem. 4 (2006) 2733–2744.
[6] P. Singh, R.H. Jayaramaiah, S.B. Agawane, G. Vannuruswamy, A.M. Korwar, A. Anand, V.S. Dhaygude, M.L. Shaikh, R.S. Joshi, R. Boppana, M.J. Kulkarni, H.V. Thulasiram, A.P. Giri, Potential dual role of eugenol in inhibiting advanced glycation end products in diabetes: Proteomic and mechanistic insights, Sci. Report. 6 (2016) 18798.
[7] B. Huang, P.L. Keeling, T.A. Hennen-Bierwagen, A.M. Myers, Comparative in vitro analyses of recombinant maize starch synthases SSI, SSIIa, and SSIII reveal direct regulatory interactions and thermo-sensitivity, Arch. Biochem. Biophys. 596 (2016) 63–72.
[8] T. Koeduka, G.V. Louie, I. Orlova, C.M. Kish, M. Ibdah, C.G. Wilkerson, M.E. Bowman, T.J. Baiga, J.P. Noel, N. Dudareva, E. Pichersky, The multiple phenylpropene synthases in both *Clarkia breweri* and *Petunia hybrida* represent two distinct protein lineages, Plant J. 54 (2008) 362–374.
[9] T. Koeduka, T.J. Baiga, J.P. Noel, E. Pichersky, Characterization of t-anol/isoeugenol synthase and an *O*-methyltransferase specific for a C7-C8 propenyl side chain, Plant Physiol. 149 (2009) 384–394.
[10] T. Min, H. Kasahara, D.L. Bedgar, B. Youn, P.K. Lawrence, D.R. Gang, S.C. Halls, H. Park, J.L. Hilsenbeck, L.B. Davin, N.G. Lewis, C. Kang, Crystal structures of pinoresinol-lariciresinol and phenylcoumaran benzylic ether reductases and their relationship to isoflavone reductases, J. Biol. Chem. 278 (2003) 50714–50723.
[11] P. Singh, R.H. Jayaramaiah, P. Sarate, H.V. Thulasiram, M.J. Kulkarni, A.P. Giri, Insecticidal potential of defense metabolites from *Ocimum kilimandscharicum* against *Helicoverpa armigera*, PLoS One 9 (8) (2014), e104377.
[12] K. Tamura, G. Stecher, D. Peterson, A. Filipski, S. Kumar, MEGA6: Molecular evolutionary genetics analysis version 6.0, Mol. Biol. Evol. 30 (2013) 2725–2729.
[13] I. Araguez, S. Osorio, T. Hoffmann, J.L. Rambla, N. Medina-Escobar, A. Granell, M.Ã. Botella, W. Schwab, V. Valpuesta, Eugenol production in achenes and receptacles of strawberry fruits is catalyzed by synthases exhibiting distinct kinetics, Plant Physiol. 163 (2013) 946–958.
[14] T. Akashi, S. Koshimizu, T. Aoki, S.I. Ayabe, Identification of cDNAs encoding pterocarpan reductase involved in isoflavan phytoalexin biosynthesis in *Lotus japonicus* by EST mining, FEBS Lett. 580 (2006) 5666–5670.
[15] M. Fujita, D.R. Gang, L.B. Davin, N.G. Lewis, Recombinant pinoresinol-lariciresinol reductases from western red cedar (*Thuja plicata*) catalyze opposite enantiospecific conversions, J. Biol. Chem. 274 (1999) 618–627.
[16] D.R. Gang, H. Kasahara, Z.Q. Xia, M.K. Vander, G. Bauw, W. Boerjan, M.M. Van, L.B. Davin, N.G. Lewis, Evolution of plant defense mechanisms: relationships of phenylcoumaran benzylic ether reductases to pinoresinol-lariciresinol and isoflavone reductases, J. Biol. Chem. 274 (1999) 7516–7527.
[17] C. Filling, K.D. Berndt, J. Benach, S. Knapp, T. Prozorovski, E. Nordling, R. Ladenstein, H. Jörnvall, U. Oppermann, Critical residues for structure and catalysis in short-chain dehydrogenases/reductases, J. Biol. Chem. 277 (2002) 25677–25684.
[18] X. Wang, X. He, J. Lin, H. Shao, Z. Chang, R.A. Dixon, Crystal structure of isoflavone reductase from alfalfa (*Medicago sativa* L.), J. Mol. Biol. 358 (2006) 1341–1352.
[19] A. Raina, A. Kumar, M. Dutta, Chemical characterization of aroma compounds in essential oil isolated from "holy basil" (*Ocimum tenuiflorum* L.) grown in India, Genet. Resour. Crop. Evol. 60 (2013) 1727–1735.
[20] Y. Iijima, R. Davidovich-Rikanati, E. Fridman, D.R. Gang, E. Bar, E. Lewinsohn, E. Pichersky, The biochemical and molecular basis for the divergent patterns in the biosynthesis of terpenes and phenylpropenes in the peltate glands of three cultivars of basil, Plant Physiol. 136 (2004) 3724–3736.
[21] M. Wink, Introduction: biochemistry, physiology and ecological functions of secondary metabolites, in: M. Wink (Ed.), Biochemistry of Plant Secondary Metabolites, Annu Plant Rev, second ed.Wiley-Blackwell, Hoboken, New Jersey 2010, pp. 1–19.
[22] Z. Xie, J. Kapteyn, D.R. Gang, A systems biology investigation of the MEP/terpenoid and shikimate/phenylpropanoid pathways points to multiple levels of metabolic control in sweet basil glandular trichomes, Plant J. 54 (2008) 349–361.
[23] P. Singh, R.M. Kalunke, A.P. Giri, Towards comprehension of complex chemical evolution and diversification of terpenoids and phenylpropanoid pathways in *Ocimum* species, RSC Adv. 5 (2015) 106886–106904.
[24] M.M.B. Zvi, E. Shklarman, T. Masci, H. Kalev, T. Debener, S. Shafir, M. Ovadis, A. Vainstein, PAP1 transcription factor enhances production of phenylpropanoid and terpenoid scent compounds in rose flowers, New Phytol. 195 (2012) 335–345.
[25] R. Dexter, A. Qualley, C.M. Kish, C.J. Ma, T. Koeduka, D.A. Nagegowda, N. Dudareva, N. Pichersky, D. Clark, Characterization of a petunia acetyltransferase involved in the biosynthesis of the floral volatile isoeugenol, Plant J. 49 (2007) 265–275.